



## Open Archive TOULOUSE Archive Ouverte (OATAO)

OATAO is an open access repository that collects the work of Toulouse researchers and makes it freely available over the web where possible.

This is an author-deposited version published in : <http://oatao.univ-toulouse.fr/>  
Eprints ID : 16677

**To link to this article** : DOI:10.1039/c6cc06137k  
URL : <http://dx.doi.org/10.1039/c6cc06137k>

**To cite this version** : Rat, Sylvain and Nagy, Venonika and Suleimanov, Iurii and Molnar, Gabor and Salmon, Lionel and Demont, Philippe and Csóka, Levente and Bousseksou, Azzedine *Elastic coupling between spin-crossover particles and cellulose fibers*. (2016) Chemical Communications, vol. 52 (n° 75). pp. 11267-11269. ISSN 1359-7345

Any correspondence concerning this service should be sent to the repository administrator: [staff-oatao@listes-diff.inp-toulouse.fr](mailto:staff-oatao@listes-diff.inp-toulouse.fr)

# Elastic coupling between spin-crossover particles and cellulose fibers

Cite this: DOI: 10.1039/c6cc06137k

S. Rat,<sup>a</sup> V. Nagy,<sup>b</sup> I. Suleimanov,<sup>a</sup> G. Molnár,<sup>a</sup> L. Salmon,<sup>a</sup> P. Demont,<sup>\*c</sup> L. Csóka<sup>b</sup> and A. Bousseksou<sup>\*a</sup>

DOI: 10.1039/c6cc06137k

**Composite materials made of cellulose fibers and spin crossover micro-particles were investigated by magnetic measurements and dynamic mechanical analysis (DMA). The storage modulus of the cellulose handsheet (0.6 GPa at room T) is significantly enhanced in the composite (1.7 GPa). The latter also displays a reversible increase of ca. 10% when switching the magnetic spin state of the particles from the low spin (LS) to the high spin (HS) form. Around the spin transition temperature a loss modulus peak is also observed, highlighting the strong viscoelastic coupling between the particles and the cellulose matrix. These results pave the way for the development of a novel family of actuator materials based on spin crossover-polymer composites.**

Spin crossover (SCO) complexes of transition metal ions<sup>1</sup> have lately received increasing attention for their mechanical properties and in particular for the possibility of harvesting a very significant volume change, which accompanies the SCO phenomenon. Indeed, this property provides remarkable prospects for the use of SCO materials in mechanical actuator technology.<sup>2</sup> The spontaneous strain during the spin transition was recently exploited through the integration of SCO materials into bimorph cantilevers, which were actuated either thermally or by light irradiation.<sup>3</sup> Strain-mediated coupling of SCO with electrical,<sup>4,5</sup> optical<sup>6</sup> and magnetic properties<sup>7–10</sup> has also been reported in hybrid SCO materials. In this context, we realize that the development of “artificial muscles” using polymer-SCO composites appears to be particularly promising. An artificial muscle is a kind of actuator generally defined by analogy with the skeletal muscle, and as stated by Tondy,<sup>11</sup> any material or device whose shape can change in response to a stimulus can potentially be a candidate for the label “artificial muscle”. This was clearly

demonstrated through the development of an electromechanical actuator made of particles of the SCO complex  $[\text{Fe}(\text{Htrz})_2(\text{trz})](\text{BF}_4)$  (Htrz = 1,2,4-*H*-triazole and trz = 1,2,4-triazole) dispersed in a poly(methylmethacrylate) matrix.<sup>12</sup> For further progress with this novel class of actuator materials, it will be, however, crucial to understand how the elastic strain associated with the spin transition is transmitted to the macroscopic scale in composite materials.

Here we report on the mechanical analysis of cellulose-SCO composites, revealing remarkable elastic strain coupling phenomena. The linter cellulose fibre composite **1** with ~50 w% loading of  $[\text{Fe}(\text{Htrz})_2(\text{trz})](\text{BF}_4)$  microparticles was prepared using a procedure described in a previous article.<sup>13</sup> The fairly homogenous distribution of SCO particles over the linter cellulose surface is clearly observed on the SEM images in Fig. 1. The magnetic properties of the composite are shown in Fig. 2. At room temperature, the composite is diamagnetic, but upon heating it becomes paramagnetic around 110–115 °C. The return to the diamagnetic phase occurs around 80 °C with a large thermal hysteresis. This behaviour corresponds to the well-known spin transition of  $[\text{Fe}(\text{Htrz})_2(\text{trz})](\text{BF}_4)$ .<sup>14</sup> The spin transition of the composite is also accompanied by a pronounced thermo-chromism between the LS (pink) and HS (white) phases.<sup>13</sup>

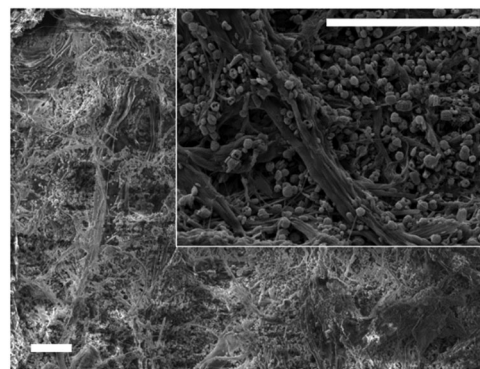


Fig. 1 SEM images of composite 1 (the inset shows a zoomed image). Scale bars are 10  $\mu\text{m}$ .

<sup>a</sup> LCC, CNRS & University of Toulouse (UPS, INPT), 205 route de Narbonne, 31077 Toulouse, France. E-mail: azzedine.bousseksou@lcc-toulouse.fr

<sup>b</sup> Institute of Wood Based Products and Technologies, University of West Hungary, 9400 Sopron, Hungary

<sup>c</sup> Institut Carnot CIRIMAT, CNRS & University of Toulouse (UPS, INPT), 118 Route de Narbonne, 31062 Toulouse, France. E-mail: demont@cict.fr

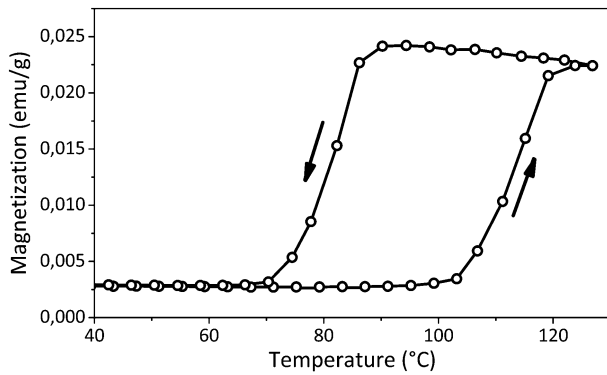


Fig. 2 Magnetization of composite 1 as a function of the temperature recorded at  $4\text{ }^{\circ}\text{C min}^{-1}$ . Arrows indicate heating and cooling.

The mechanical properties of the composite and pure cellulose handsheets were characterized by DMA, wherein an oscillatory force (stress) is applied to a material and the resulting displacement (strain) is measured. An ARES G2 rheometer from TA Instruments was used in tensile mode in the temperature range between 55 and  $130\text{ }^{\circ}\text{C}$  with heating/cooling rates of  $2\text{ }^{\circ}\text{C min}^{-1}$ , a preload force of 0.7 N, a static force/dynamic force amplitude ratio (“force tracking”) of 120%, and an oscillation frequency of 1 Hz. Samples were cut in a rectangular shape ( $25 \times 7\text{ mm}$ ), with an approximate thickness of  $170\text{ }\mu\text{m}$ , and were loaded at a starting gap height of 10 mm between the clamps. The composite was cycled several times before reaching stability. Preliminary tests were performed at  $23\text{ }^{\circ}\text{C}$  in a dry nitrogen atmosphere to determine optimal mechanical conditions as well as stress–strain curves (Fig. 3). The latter indicate a reinforcement, *i.e.* higher stiffness of the handsheets loaded with SCO particles. The slope of the stress–strain curves below  $\sim 0.1\%$  strain gives the Young’s modulus, which increases from 0.6 GPa for the pure cellulose to 1.7 GPa for composite 1. Besides the intrinsically higher stiffness of the SCO material, one may suggest that the SCO particles also affect the free OH groups of the cellulose and thus participate in inter-fibre hydrogen bonding, which in turn increases the stiffness of the network.<sup>15,16</sup> Hence the reinforcement imparted by the  $[\text{Fe}(\text{Htrz})_2(\text{trz})](\text{BF}_4)$  particles allows greater stress transfer from the cellulose to the SCO particles at the interface.

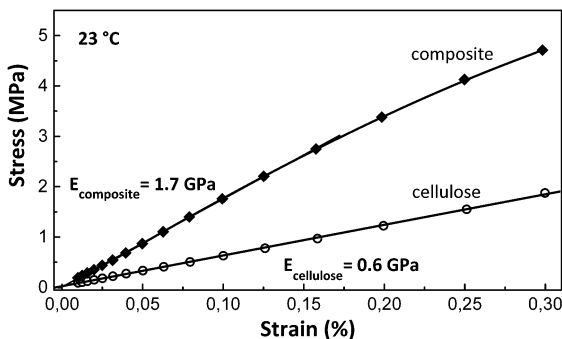


Fig. 3 Stress–strain curves of the pure and composite cellulose sheets at  $23\text{ }^{\circ}\text{C}$ . The error bars are smaller than the symbol size.

Application of a dynamic, vibrational load to paper sheets will result in a combination of elastic and viscous responses. Various theoretical approaches were suggested to model this behaviour. Researchers usually employ linear and non-linear continuum models in order to explain stress relaxation and creep, since these are the standard methods for investigation of paper viscoelastic properties.<sup>17–21</sup> In the visco-elastic model the dynamic modulus  $E^*$  is the ratio of stress to strain under vibratory conditions defined as:<sup>22</sup>

$$E^* = E' + iE''$$

The real part  $E'$ , the storage modulus (elastic response), is proportional to the energy stored by the material upon reversible elastic deformation. The imaginary part  $E''$ , the loss modulus (viscous response), is proportional to the energy dissipated as heat (mainly) by the friction of macromolecular chains. The latter is an irreversible phenomenon. Fig. 4 shows the temperature dependence of the storage and loss moduli of the pure cellulose and composite sheets for a complete heating–cooling cycle. As can be expected, the storage modulus of the pure cellulose sheet exhibits a gradual decrease while increasing the temperature from 55 to  $130\text{ }^{\circ}\text{C}$ . This phenomenon is mostly related to the increase in polymer chain mobility at higher temperatures. While the magnitude of the storage modulus obviously depends on the type of fibre and its refining state, the decreasing storage modulus is a general tendency.<sup>15</sup>

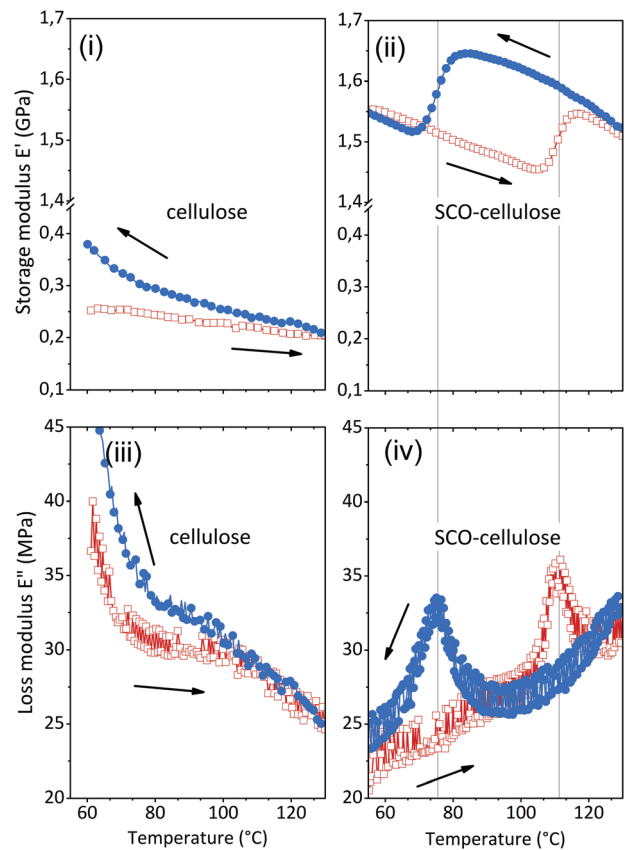


Fig. 4 Storage and loss moduli of the pure (i and iii) and composite (ii and iv) cellulose sheets at different temperatures in the heating (red open symbols) and cooling (blue closed symbols) modes. Arrows indicate heating and cooling.

The composite sheets display a similar monotonous decrease of the storage modulus up to *ca.* 110 °C, wherein  $E'$  abruptly increases by *ca.* 10%. Upon cooling, these phenomena are reversible with a decrease of  $E'$  around 80 °C. This hysteresis of the elastic modulus in Fig. 4(ii) is obviously correlated with the magnetic properties (Fig. 2). We can thus conclude that the spin transition leads to a reversible change in elastic properties of the whole cellulose composite. At first glance, the increase of the storage modulus in the HS state of the composite might seem to be surprising since the stiffness of the SCO material itself decreases at the same time.<sup>23</sup> However, one should also consider that the volume fraction of the spin crossover particles increases by *ca.* 11% while going from the LS to the HS state.<sup>24</sup> The strain induced by this volume change on the cellulose fibres seems to be the main contribution to the storage modulus increase upon the SCO in this particular case.

In addition to the elastic response to time dependent stress, irreversible plastic deformation and associated energy dissipation will also take place in the composite – mainly due to the mechanical relaxation processes of the cellulose fibres as they are stretched. These phenomena are reflected by the loss modulus whose temperature dependence is also shown in Fig. 4 for the two samples. The  $E''$  curve of the sheet made from the as received cellulose fibres shows a decrease of the loss modulus with increasing temperature. According to the results obtained by Roylance *et al.*, this tendency can be associated with the high temperature part of a broad mechanical relaxation centred around –50 °C which is related to the relaxation of restricted amorphous chains in the crystalline phase of cellulose.<sup>25</sup> The mechanical losses are weak between 80 and 130 °C, indicating that no significant relaxation occurred in this range reflected also by the weak temperature dependence of  $E''$ . The  $E''$  curves of the composite material reveal two well defined loss peaks around the spin transition temperatures. These two peaks can be assigned to heat dissipation due primarily to the friction of cellulose fibres during the spin transition.

In summary, DMA analysis revealed an abrupt and reversible stiffening of the cellulose–[Fe(Htrz)<sub>2</sub>(trz)](BF<sub>4</sub>) composite when going to the high temperature HS phase and an associated peak in the mechanical losses. These results demonstrate that it is possible to combine the functionality of compliant, free-standing polymer materials with the actuating force arising upon the spin transition in SCO particles. This approach thus provides access to functionalities (*e.g.* manufacturability), which are not easily attainable with monolithic spin crossover materials and, *vice versa*, it also allows endowing the matrix with advanced mechanical and optical properties. As a perspective, it is important to notice that by simply changing the filler microstructure (particle shape, arrangement, *etc.*) one may obtain very different mechanical couplings with the matrix. In the case of highly oriented

high aspect ratio particles, one may even anticipate opposite responses (*i.e.*  $\Delta E_{\text{HS-LS}'} > 0$  or  $\Delta E_{\text{HS-LS}'} < 0$ ) depending on the direction in which the force is applied to the composite. The empirical Halpin–Tsai equations<sup>26</sup> may provide a very useful frame for the design of these systems with tailored mechanical responses.

## Notes and references

- 1 P. Gütlich, A. Hauser and H. Spiering, *Angew. Chem., Int. Ed. Engl.*, 1994, **33**, 2024–2054.
- 2 M. D. Manrique-Juárez, S. Rat, L. Salmon, G. Molnár, C. M. Quintero, L. Nicu, H. J. Shepherd and A. Bousseksou, *Coord. Chem. Rev.*, 2016, **308**(part 2), 395–408.
- 3 H. J. Shepherd, I. A. Gural'skiy, C. M. Quintero, S. Tricard, L. Salmon, G. Molnár and A. Bousseksou, *Nat. Commun.*, 2013, **4**, 2607.
- 4 Y.-S. Koo and J. R. Galán-Mascarós, *Adv. Mater.*, 2014, **26**, 6785–6789.
- 5 Y.-C. Chen, Y. Meng, Z.-P. Ni and M.-L. Tong, *J. Mater. Chem. C*, 2015, **3**, 945–949.
- 6 I. Suleimanov, O. Kraieva, J. S. Costa, I. O. Fritsky, G. Molnár, L. Salmon and A. Bousseksou, *J. Mater. Chem. C*, 2015, **3**, 5026–5032.
- 7 N. Dia, L. Lisnard, Y. Prado, A. Gloter, O. Stéphan, F. Brisset, H. Hafez, Z. Saad, C. Mathonière, L. Catala and T. Mallah, *Inorg. Chem.*, 2013, **52**, 10264–10274.
- 8 O. N. Risset, P. A. Quintero, T. V. Brinzari, M. J. Andrus, M. W. Lufaso, M. W. Meisel and D. R. Talham, *J. Am. Chem. Soc.*, 2014, **136**, 15660–15669.
- 9 C. R. Gros, M. K. Pehrah, B. D. Hosterman, T. V. Brinzari, P. A. Quintero, M. Sendova, M. W. Meisel and D. R. Talham, *J. Am. Chem. Soc.*, 2014, **136**, 9846–9849.
- 10 M. Presle, I. Maurin, F. Maroun, R. Cortès, L. Lu, R. Sayed Hassan, E. Larquet, J.-M. Guigner, E. Rivière, J. P. Wright, J.-P. Boilot and T. Gacoin, *J. Phys. Chem. C*, 2014, **118**, 13186–13195.
- 11 B. Tondou, *Actuators*, 2015, **4**, 336–352.
- 12 I. A. Gural'skiy, C. M. Quintero, J. S. Costa, P. Demont, G. Molnár, L. Salmon, H. J. Shepherd and A. Bousseksou, *J. Mater. Chem. C*, 2014, **2**, 2949.
- 13 V. Nagy, I. Suleimanov, G. Molnár, L. Salmon, A. Bousseksou and L. Csóka, *J. Mater. Chem. C*, 2015, **3**, 7897–7905.
- 14 J. Kröber, J.-P. Audière, R. Claude, E. Codjovi, O. Kahn, J. G. Haasnoot, F. Grolière, C. Jay and A. Bousseksou, *Chem. Mater.*, 1994, **6**, 1404–1412.
- 15 L. Csóka, D. K. Božanić, V. Nagy, S. Dimitrijević-Branković, A. S. Luyt, G. Grozdits and V. Djoković, *Carbohydr. Polym.*, 2012, **90**, 1139–1146.
- 16 V. Nagy, K. Halász, M.-T. Carayon, I. A. Gural'skiy, S. Tricard, G. Molnár, A. Bousseksou, L. Salmon and L. Csóka, *Colloids Surf., A*, 2014, **456**, 35–40.
- 17 J. Alifthan, *Mech. Time-Depend. Mater.*, 2004, **8**, 289–302.
- 18 J. Alifthan, *Nord. Pulp Pap. Res. J.*, 2010, **25**, 351–357.
- 19 A. DeMaio and T. Patterson, *Mech. Time-Depend. Mater.*, 2006, **10**, 17–33.
- 20 A. DeMaio and T. Patterson, *J. Appl. Polym. Sci.*, 2007, **106**, 3543–3554.
- 21 M. Mustalahti, J. Rosti, J. Koivisto and M. J. Alava, *J. Stat. Mech.: Theory Exp.*, 2010, **2010**, P07019.
- 22 R. E. Mark and J. Borch, *Handbook of Physical Testing of Paper*, CRC Press, 2001.
- 23 G. Félix, M. Mikolasek, H. Peng, W. Nicolazzi, G. Molnár, A. I. Chumakov, L. Salmon and A. Bousseksou, *Phys. Rev. B: Condens. Matter Mater. Phys.*, 2015, **91**, 24422.
- 24 A. Grosjean, P. Négrier, P. Bordet, C. Etrillard, D. Mondieig, S. Pechev, E. Lebraud, J.-F. Létard and P. Guionneau, *Eur. J. Inorg. Chem.*, 2013, 796–802.
- 25 D. Roylance, P. McElroy and F. McGarry, *Fibre Sci. Technol.*, 1980, **13**, 411–421.
- 26 J. C. H. Affdl and J. L. Kardos, *Polym. Eng. Sci.*, 1976, **16**, 344–352.